Journal of Sound and Vibration (2001) **241**(2), 235–245
doi:10.1006/jsvi.2000.3299, available online at http://www.idealibrary.com on IDEAL®

DAMPING FACTOR AS AN INDICATOR OF CRACK SEVERITY

S. D. Panteliou, T. G. Chondros and V. C. Argyrakis

Machine Design Laboratory, Department of Mechanical Engineering and Aeronautics, University of Patras, Patras 265 00, *Greece. E-mail: panteliu@mech.upatras.gr*

AND

A. D. Dimarogonas

W. Palm Professor of Mechanical Design, Washington University, St. Louis, MO 63130, *U.S.A.*

(*Received* 28 *September* 1999, *and in final form* 26 *July* 2000)

When a material is subjected to an alternating stress field there are temperature fluctuations throughout its volume due to thermoelastic effect. The resulting irreversible heat conduction leads to entropy production, which in turn is the cause for thermodynamic damping. An analytical investigation of the entropy produced during a vibration cycle due to the reciprocity of temperature rise and strain yielded the change of the material damping factor as a function of shape and magnitude of existing crack in the structure. A homogeneous, isotropic, elastic bar of orthogonal shape is considered with a single-edge crack under alternating uniform axial stress. The analytical determination of the dynamic characteristics of the cracked structure yielded the damping factor of the bar, the material damping factor and a good correlation of depth of crack with the damping factor. Experimental results on cracked bars are in good correlation with the analysis.

1. INTRODUCTION

It is well known that the existence of a crack in a structure is related to the decrease in its strength. The evaluation of the effect of cracks on the strength of the material, especially in relation with fatigue and brittle fracture is a very important consideration in engineering design. Numerous researchers have investigated crack identification extensively. A thorough state of the art review can be found in reference [1].

Barenblatt *et al.* [2], while dealing with the influence of the vibrational heating on the fracture propagation in polymeric materials, considered that the failure process for rigid cracked materials is localized at the crack tips, where stress concentration takes place. Therefore, the intensity of heat generation, which is proportional to the square of the stress amplitude is low, far from the crack tips, but might be considerable and involve a substantial temperature rise near the crack tips. Thus, due to the vibrational stress, a non-uniform temperature distribution in the sample arises, activating the failure process (rupture of bonds) just in the places where it is localized. In the remaining part of the sample the temperature rise is usually negligible. These considerations gave a complete quantitative theory for the local heating effect on the rate of the crack propagation. Specifically, they gave analytical expressions for the stress and temperature fields in the cracked structure.

0022-460X/01/120235 + 11 $35.00/0

Damping is also a very important material and structural property when dealing with vibrating structures from the point of view of vibration attenuation in cracked structures. For a material, there are many damping mechanisms [3], most of which contribute significantly to the total damping only over a certain narrow range of frequency, temperature or stress. Among them, thermodynamic damping is due to the non-reversible heat conduction in the material.

Zener first studied thermodynamic damping for transverse vibrations of homogeneous Euler–Bernoulli beam [4]. The case of general homogeneous medium was investigated by Biot [5], Lucke [6], Deresiewicz [7], Alblas [8, 9], and Gillis [10], while the case of homogeneous plates, shells and Timoshenko beams were investigated by Tasi [11], Tasi and Herrmann [12], Shieh [13–15] and Lee [16]. The connection between the second law of thermodynamics and thermodynamic damping was also discussed by Goodman *et al.* [17], and Landau and Lifshitz [18]. Armstrong [19] calculated thermodynamic damping of one-dimensional composite consisting of successive slabs assuming identical thermal conductivity and specific heat for all slabs. Kinra and Milligan [20] presented a general methodology for calculating thermodynamic damping in homogeneous or composite materials. Milligan and Kinra [21] extended the calculation to a single linear inclusion in an unbounded matrix. The case of an Euler–Bernoulli beam was examined by Bishop and Kinra [22]. Bishop and Kinra [23] investigated the thermodynamic damping of a laminated beam in flexure and extension. Bishop and Kinra [24] calculated the thermodynamic damping of an N-layer metal matrix composite in a Cartesian, cylindrical and spherical coordinate system with perfect or imperfect thermal interfaces. Milligan and Kinra [25] calculated the thermodynamic damping of a fibber reinforced metal–matrix composite.

In this paper, the thermodynamic damping of a homogeneous, isotropic, elastic bar with a single-edge surface crack under alternating uniform axial stress is calculated analytically and experimentally and the associated damping factor is related to the depth of the crack.

2. ANALYTICAL MODEL

The thermomechanical behaviour of a linear, isotropic and homogeneous thermoelastic medium is described by the following equations: the first law of thermodynamics [26]

$$\rho \partial u/\partial t = \sigma_{ij} \partial e_{ij}/\partial t - q_{ij}, \tag{1}$$

Newton's law of motion-conservation of linear momentum [27],

$$\sigma_{ji,j} = \rho \partial^2 u_i/\partial t^2, \tag{2}$$

the kinematic equations of linear thermoelasticity–strain displacement relations [28],

$$e_{ij} = 1/2(u_{i,j} + u_{j,i}), \tag{3}$$

the second law of thermodynamics [26],

$$\rho \partial s/\partial t + (q_i/T)_i \geqslant 0, \tag{4}$$

the thermoelastic Hooke's law [28],

$$\sigma_{ij} = E/(1 + v)(e_{ij} + v/(1 - 2v)e_{kk}\delta_{ij} - E/(1 - 2v)\alpha_l \delta_{ij}(T - T_0), \tag{5}$$

the Fourier law of heat conduction [29],

$$q_i = -kT_{,i}. \tag{6}$$

Here σ_{ij} is the stress tensor, e_{ij} is the strain tensor, u_i is the displacement vector, v is the Poisson ratio, E is Young's modulus, ρ is the density, s is the entropy produced per unit mass, T is the absolute temperature, T_0 is the thermodynamic equilibrium temperature, q_i is the heat flux vector, u is the internal energy per unit mass, δ_{ij} is the Kronecker delta, k is the thermal conductivity, α_l is the coefficient of thermal expansion and the indices i, j, k each have a value of 1, 2 and 3.

From the above equations the relation between temperature and strain is [27]

$$T_{,ii} - (\rho c/k)\,\partial T/\partial t = [E\alpha_l/k(1-2v)]\,T\,\partial e_{kk}/\partial t. \tag{7}$$

In this equation, the term $(T\partial e_{kk}/\partial t)$ couples the temperature field with the mechanical field and leads to a nonlinear problem. One can replace T on the right-hand side of equation (7) with the thermodynamic equilibrium temperature T_0, because the fluctuations in temperature caused by reasonable alternating stress levels are very small. This assumption linearizes the differential equation. Equation (7) shows that for an isotropic material [30],

$$(\partial T/\partial \sigma_{kk})_S = -T\alpha_l/C, \tag{8}$$

where C is the specific heat per unit volume. Since the temperature and mechanical fields are coupled, inhomogeneities in stress and material properties result in inhomogeneities in temperature. Heat is conducted from the high-temperature regions to the low-temperature regions and, as a consequence of the second law of thermodynamics, entropy is produced which is manifested as a conversion of useful mechanical energy into heat.

When the second law of thermodynamics is applied to heat conduction in solids, it results in the calculation of the flow of entropy produced per unit volume $\dot{s}_p = \mathrm{d}s_p/\mathrm{d}t$ due to irreversible heat conduction [31, 32] as

$$\dot{s}_p = k/(\rho T_0^2)(\partial T/\partial r)^2. \tag{9}$$

The elastic energy W_{el} stored per unit volume and cycle of vibration is [33]

$$W_{el} = (1/2E)\,(\sigma_{xx}^2 + \sigma_{yy}^2 + \sigma_{zz}^2) - (v/E)\,(\sigma_{xx}\sigma_{yy} + \sigma_{yy}\sigma_{zz} + \sigma_{zz}\sigma_{xx}). \tag{10}$$

The entropy Δs produced per unit volume and cycle of vibration is

$$\Delta s = \oint T_p\,\dot{s}_p\,\mathrm{d}t, \tag{11}$$

where T_p is the period of vibration.

From the Gouy–Stodola theorem [34–36] the mechanical energy $\dot{W}$ dissipated per unit of volume and per unit of time is

$$\dot{W} = \rho T_0\,\dot{s}_p. \tag{12}$$

The mechanical energy ΔW dissipated per cycle of vibration in a medium of volume V is

$$\Delta W = \rho T_0 \int_V \Delta s\,\mathrm{d}V. \tag{13}$$

Equation (13) relates the entropy produced in the material during one cycle of vibration to the elastic energy dissipated.

Finally, the *material damping factor* γ is defined as the energy dissipated throughout the medium in one cycle, normalized with respect to the maximum elastic energy stored during that cycle [37]:

$$\gamma = \Delta W/4\pi \int_V W_{el}\, \mathrm{d}V. \tag{14}$$

The *modal damping factor* ζ is defined [37] as

$$\zeta = \sqrt{(\gamma^2/(4 + \zeta^2)}. \tag{15}$$

From equation (3.63) on p. 154 of reference [37]

$$2\zeta/\sqrt{(1 - \zeta^2)} \cong 2\zeta = \omega_n/\omega = \gamma \tag{15a}$$

and hence for natural vibration $\omega/\omega_n = 1$ and $\delta/\pi = \gamma \cong 2\zeta$

$$\gamma = 2\zeta. \tag{15b}$$

Then raising to the second power on both sides of equation (15) one obtains

$$\zeta^2 = (\gamma^2/(4 + \zeta^2) \Rightarrow \zeta^2 + \zeta^4 = \gamma^2. \tag{15c}$$

From equations (15b) and (15c) $\zeta^4 = 0$, which is true, given that ζ is very small. Hence, equation (15) is valid.

Equations (1)–(15) show the relationship between the stress field and the material or the modal damping factor of the bar due to the thermoelastic effect.

3. CRACK IDENTIFICATION FROM THE INFLUENCE OF VIBRATIONAL HEATING

To improve our understanding of the mechanism of energy conversion and the relation of the cyclic stresses to the vibration damping, analytical and experimental work in cracked structures has been carried out.

Consider a homogeneous, isotropic, elastic bar with a single-edge surface crack under alternating uniform axial load P, as shown in Figure 1. According to the basic concept of Zhurkov [38, 39], the fracture of solids is a process which takes place in time under any stress, is controlled by certain kinetics due to thermal fluctuations and is strongly affected by temperature and stress.

Barenblatt *et al.* [2], considering the local heating effect on the rate of the crack propagation, gave analytical expressions for the stress and temperature fields in a cracked structure. They supposed that the period of vibrations is sufficiently small in comparison with the characteristic time of the temperature change. In this case, the heat transfer equations are solved and averaged over a time interval sufficiently large as compared with the time of substantial change of temperature. The failure process takes place mainly in a region near the crack edge with linear dimensions of the order of d (see Figure 1), which is

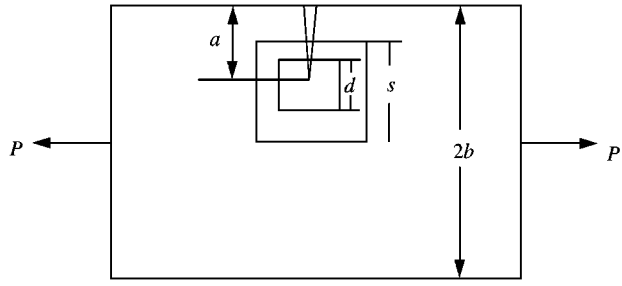

Figure 1. Elastic bar with a single-edge surface crack under alternating uniform axial load P.

assumed small in comparison with the characteristic length (crack length a). Then, according to reference [2], the stresses at any point are

$$\sigma_{xx}^a = N_0^a r^{-1/2} \cos(\theta/2)\,[1 - \sin(\theta/2)\sin(3\theta/2)],$$

$$\sigma_{yy}^a = N_0^a r^{-1/2} \cos(\theta/2)\,[1 + \sin(\theta/2)\sin(3\theta/2)],$$

$$\sigma_{zz}^a = 2\nu N_0^a r^{-1/2} \cos(\theta/2),$$

$$\tau_{xy}^a = N_0^a r^{-1/2} \cos(\theta/2)\sin(\theta/2)\cos(3\theta/2),$$

$$\tau_{xz}^a = \tau_{yz}^a = 0, \tag{16}$$

while the temperature distribution close to the crack tip is

$$T(r,\theta) = T_0 + \omega I''(N_0^a)^2/4\pi k \int_0^{2\pi}$$

$$\times \int_0^{\infty} [\mathrm{K}_0(\eta\zeta)\,\Psi(\theta'')\,\mathrm{e}^{\kappa\zeta\cos\theta}\,\zeta\,\mathrm{d}\zeta\,\mathrm{d}\theta'/\sqrt{(\zeta^2 - 2r\zeta\cos(\theta' - \theta))}], \tag{17}$$

In the above equations N_0^a is the amplitude of the stress intensity factor, r is the distance of the considered point from the crack tip, θ is the polar angle, ν is the Poisson ratio, $T(r, \theta)$ is the temperature at any point (r, θ), T_0 is the ambient temperature, ω is the frequency of vibration, I'' is the loss compliance, k is the thermal conductivity, K_0 is the modified Bessel function, $\eta = (\kappa^2 + \alpha^2)^{1/2}$, $\kappa = u/2a_{diff}$, u is the velocity with which the crack tip moves along the x-axis, $a_{diff} = k/\rho c$ the thermal diffusivity, ρ the density, c the specific heat, $\alpha = (h/k)^{1/2}$ and h is the convection heat transfer coefficient. According to equation (17), the temperature at any point (r, θ), is derived from the integral of the impact of the temperature of every other point on the specific point. The local geometry is presented in Figure 2, where ζ, θ' and θ'' are shown. Also from reference [2]

$$\Psi(\theta) = 11/8 + 2\nu^2 + (11/8 + 2\nu^2)\cos\theta - 3/8\cos^2\theta - 7/8\cos^3\theta + 1/2\cos^5\theta. \tag{18}$$

At this point, the stress and temperature fields can be computed from equations (16–18). The mechanical energy ΔW dissipated in the solid per cycle of vibration is derived from equations (9), (11) and (13) with temperatures calculated from equations (17) and (18) by

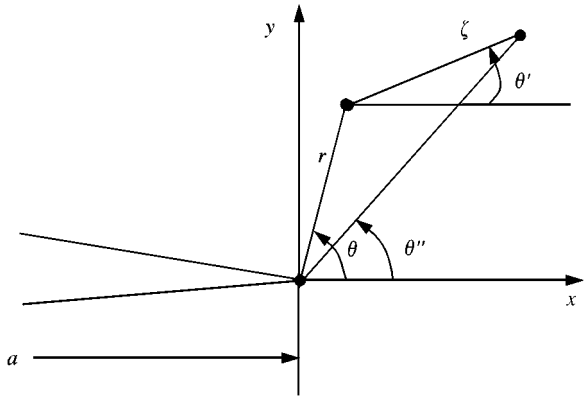

Figure 2. Local crack geometry.

a finite difference method at a lattice of points (i, j), where the integration is replaced with summation by using the trapezoidal rule

$$\Delta W = kT_p/4T_0 Z s \left[\left(\sum_{i=1}^{n} (T_{i+1,j} - T_{i-1,j})^2 \right) \Big/ \Delta x + \left(\sum_{i=1}^{n} (T_{i,j+1} - T_{i,j-1})^2 \right) \Big/ \Delta y \right], \quad (19)$$

where $Tp = 2\pi/\omega$ is the period of vibration, Z is the bar width and s is the linear dimension of the rectangular region near the crack edge, where the heat generation process and flow mainly take place. Δx, Δy are the mesh spacings in the x- and y-axis respectively.

The total elastic energy $W_{elastic}$ of elastic deformation per cycle of vibration in the volume V of the solid is, as calculated from equation (10),

$$W_{elastic} = \int_V W_{el} \, \mathrm{d}V \quad (20)$$

while the damping factor γ and the modal damping factor ζ are calculated from equations (14) and (15) respectively.

A numerical application was performed for the following bar and crack geometry, technical characteristics and material properties, for bars made out of Plexiglas: length of the bar $1 = 0{\cdot}236$ m, cross-section height $2b = 0{\cdot}022$ m, cross-section width $Z = 0{\cdot}009$ m, velocity of crack propagation $u = 0$ m/s, ambient temperature $T_0 = 25°\mathrm{C}$, frequency of vibration $\omega = 4{\cdot}2$ kHz, Young's modulus $E = 3{\cdot}1026 \times 10^9$ N/m^2 [40], Poisson's ratio $v = 0{\cdot}35$ [40], density $\rho = 1190$ kg/m^3 [40], coefficient of thermal expansion $\alpha_1 = 0{\cdot}0000738$ m/m °C [40], thermal conductivity $k = 0{\cdot}18749$ W/m °C [40], specific heat $C = 1465{\cdot}38$ J/kg °K [40], loss compliance, $I'' = 3\text{e-}9$ m^2/N [41], heat transfer coefficient $h = 21{\cdot}297593$ W/m^2 °C [42]. The amplitude of stress intensity factor has been calculated for different a/b ratios from reference [43].

The linear dimension s of the region near the crack tip, where the heating is important, leads to a mesh spacing Δx, Δy used during the application of finite differences in order to find temperatures and stresses. At this point, Barrenblatt *et al.* [2] who introduced this concept, did not define the heating region dimension s (see Figure 1) other than by the inequality

$$d \ll s \ll l. \quad (21)$$

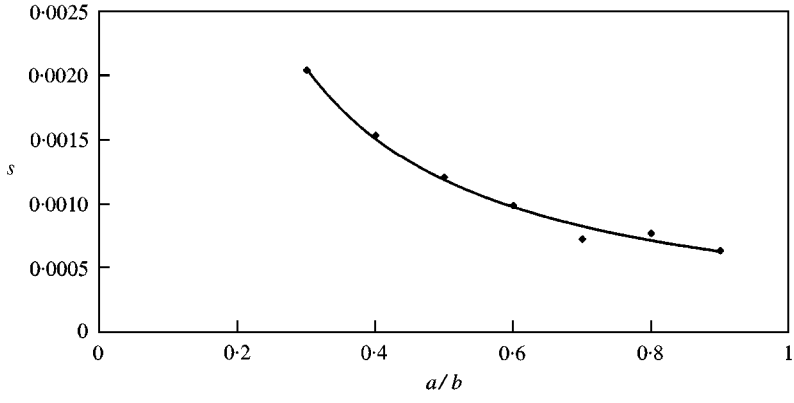

Figure 3. Correlation for linear dimension s with a/b.

We treated here the region measure s as a parameter to be experimentally identified. If it is determined for a crack of a specific geometry, it can be used for any crack location and boundary conditions of the crack signature, due to inequality (21). An empirical function was derived to relate s with a/b changes. This function was determined experimentally to be, for the particular crack geometry,

$$s = 0{\cdot}0006(a/b)^{-1{\cdot}0692} \tag{22}$$

This function was found from the demand that there should be an agreement between the analytical and experimental results for the cracked beam damping. The variation of the grid spacing is expressed in Figure 3, where the linear dimension s is plotted against the crack length ratio a/b, with correlation coefficient $R^2 = 0{\cdot}9789$. The correlation measures the relationship between the two data sets that are scaled to be independent of the unit of measurement. The population correlation calculation gives the covariance of the two data sets divided by the product of their standard deviations. Correlation can be used to determine whether two data sets move together; that is whether large values of one set are associated with large values of the other (positive correlation), whether small values of one set are associated with large values of the other (negative correlation), or whether values in both sets are unrelated (correlation near zero). The mesh spacings Δx and Δy, occurring from the linear dimension s, which is as defined in equation (22), are applied further for the calculation of the temperature field and the dissipated energy.

The analytically calculated damping factor is plotted against the crack-length ratio a/b, in Figure 4, in comparison with the experimental results obtained. It is apparent that the damping increases with increasing crack length as expected.

4. EXPERIMENTAL EVIDENCE

On the basis of the results shown in Figure 4, it is apparent that the damping change due to the existence of the crack will be substantial. To test this hypothesis, changes in modal damping were evaluated experimentally. Prismatic bars made of Plexiglas [40] of rectangular cross-section 9×22 mm and length 236 mm were prepared. At mid-span, a sharp notch was introduced, perpendicular to the longitudinal axis and the longer dimension of the cross-section. Then, the bar was placed on a heating device and the side

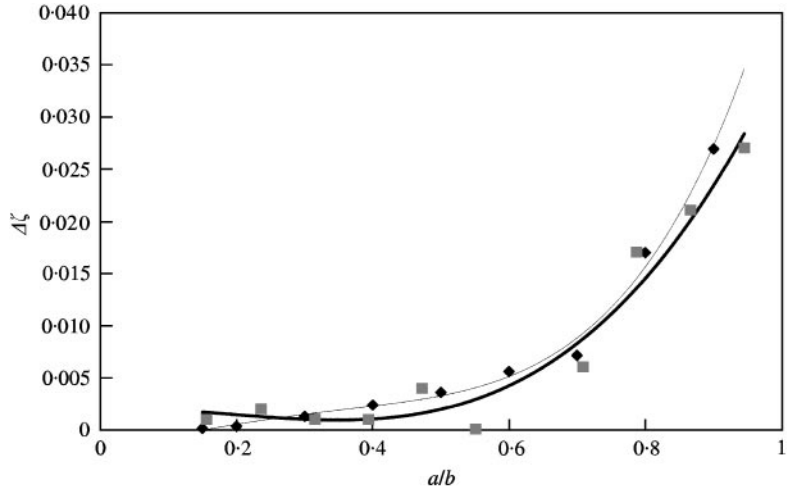

Figure 4. Material damping factor versus crack-length ratio a/b. Analytical and experimental results. (◆), $\Delta\zeta$-anal; (■), $\Delta\zeta$-exp; (—), $\Delta\zeta$-exp; (·····), $\Delta\zeta$-anal.

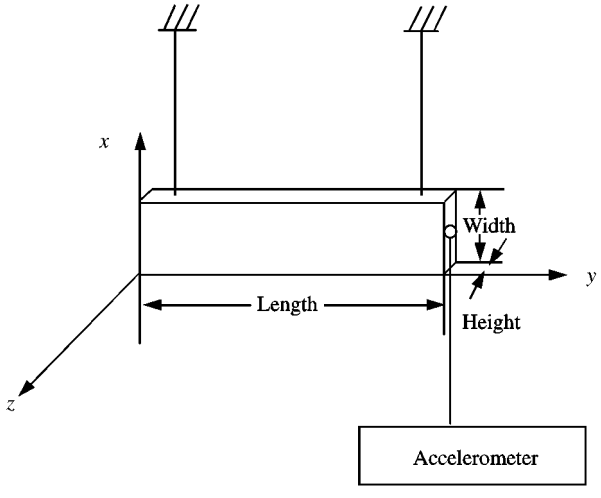

Figure 5. Experimental set-up.

opposite to the notch was heated, so that the heating was propagating towards the notch and reached a predefined point on the cross-section. Then, the specimen was removed from the heater and was hit at one end, the other being fixed, so that a crack, starting from the notch, propagated up to the heated part of the cross-section. Different specimens with varying crack lengths were obtained with this procedure.

The experimental set-up is shown in Figure 5. Each bar was supported at the two ends by thin strings to assure free longitudinal motion. An axial accelerometer of 1 g mass was fixed on the right end of the bar to measure the longitudinal frequencies in the y-direction. The bar was set into free longitudinal vibration from the initial position by hitting it with a miniature hammer at the left end in the y-direction. As is shown in Figure 5, y is the longitudinal axis of the bar considered. Although coupling of flexural and longitudinal vibration may appear, the identification of longitudinal frequencies is facilitated by the fact

that flexural and longitudinal vibration frequencies are well separated. The lowest flexural vibrations in both x and z directions are below 1 kHz, while the longitudinal frequency is around 4 kHz. The response was measured directly at the same position, through the accelerometer. The output of the latter after amplification was introduced through a Data Acquisition Card (Omega OMB-DAQBOOK-100/-120/-200) to a PC and stored for further analysis. The vibration frequency was calculated by measuring the time elapsed for 50 cycles of vibration. Moreover, an FFT transform was performed at the stored signal for an independent measurement of the longitudinal natural frequencies. The lowest natural frequency of the uncracked bars was around 4·2 kHz. The 100 kHz sampling rate two-channel A/D converter used could give good accuracy for the fundamental frequency measurements.

Measurements were taken for crack depths up to 90% of the cross-section half height b, which is of importance for engineering applications. Also, the experimental points are averages from the tests, though the spread of frequency measurements about the points was very small.

The vibration modal damping factor ζ (MDF) was obtained by applying the logarithmic decrement method [37]. Ten independent measurements of the damping factor have been performed on each bar to yield, from their average, the damping measurement of the cracked structure for every crack length ratio a/b. This damping value accounts for the crack only and is compared with the analytical results in Figure 4.

5. CONCLUSIONS

The thermodynamic theory of damping was used to find the material damping due to the crack, which results in an additional damping mechanism due to the non-reversible flow of heat from areas of higher heat generation to others of lower heat generation. This was further related to the crack depth.

Our analysis and experiments are limited to elastic strains and frequencies, leading to the production of change in the damping factor which depends on the crack length and thus becomes a material and a system property. Solution for the bar with a single edge was employed.

The damping factor increases with increasing crack-length ratio a/b, as shown in Figure 4. The change from the uncracked bar to the one cracked to half its thickness ($a/b = 1$) is about 4% which is measurable, since the standard deviation in our damping measurements was about 1%. Moreover, it is known that thermodynamic damping is very low, as compared with other damping mechanisms [44, 45]. However, the measurement of its change with the depth of the crack apparently correlates well with the crack depth.

This analysis can be used in a number of engineering problems.

1. As a continuous quality control tool for the production of ceramics, glass and similar materials that their quality is diminished, with, even, initiating cracks.
2. As a design tool for crack identification in structures.
3. In the biomedical field, as part of a diagnostic and monitoring tool for cracked bones and other conditions of bone loss.

The proposed crack identification method is as sensitive as the spectral method (measurement of the change in natural frequency), but has the advantage that, unlike the spectral method, it is relatively insensitive to the change or uncertainty in the boundary conditions. Besides, for any known material it does not require an initial base-line measurement of damping on the cracked structure.

REFERENCES

1. A. D. DIMAROGONAS 1996 *Engineering Fracture Mechanics* **55**, 831–857. Vibration of cracked structures: a state of the art review.
2. G. I. BARENBLATT, V. M. ENTOV and R. I. SALGANIK 1968, 33–46. *On the Influence of Vibrational Heating on the Fracture Propagation in Polymeric Materials*. Moscow (U.S.S.R).
3. B. J. LAZAN 1968 *Damping of Materials and Members in Structural Mechanics*. Oxford: Pergamon Press.
4. C. ZENER 1937 *Physical Review* **52**, 230–235.
5. M. BIOT 1956 *Journal of Applied Physics* **27**, 240–253.
6. K. LUCKE 1956 *Journal of Applied Physics* **27**, 1433–1438. Ultrasonic attenuation caused by thermoelastic heat flow.
7. H. DERESIEWITCZ 1957 *Journal of the Acoustical Society of America* **29**, 204–209. Plane waves in a thermoelastic solid.
8. J. ALBLAS 1961 *Applied Scientific Research* **A 10**, 349–367. On the general theory of thermo-elastic friction.
9. J. ALBLAS 1981 *Journal of Thermal Stresses* **4**, 333–355. A note on the theory of thermoelastic damping.
10. W. GILLIS 1968 *Technical Memorandum X*-53722, *George C. Marshall Space Flight Center*. Orbital mechanics section. Damping of thermoelastic structures.
11. J. TASI 1963 *Journal of Applied Mechanics* **30**, 562–567. Thermoelastic dissipation in vibrating plates.
12. J. TASI and G. HERRMANN 1964 *Journal of the Acoustical Society of America* **36**, 100–110.
13. R. SHIEH 1971 *NASA TND*-6448 *NASA Langley Research Center*, *Hampton Virginia*. Thermoelastic damping and it's effect on flutter of stressed panels situated in a supersonic airflow.
14. R. SHIEH 1975 *ASME Journal of Applied Mechanics* **42**, 405–410. Thermoelastic vibration and damping for circular Timoshenko beams.
15. R. SHIEH 1979 *ASME Journal of Applied Mechanics* **46**, 169–174. Eigensolutions for coupled thermoelastic vibrations of Timoshenko beams.
16. U. LEE 1985 *American Institute of Aeronautics and Astronautics Journal* **23**, 1783–1790. Thermoelastic and electromagnetic damping analysis.
17. L. GOODMAN, C. CHANG and A. ROBINSON 1962 *Technical Documentary Report No. ASD-TDR*-62-1031 *Wright-Patterson Air Force Base*, Ohio. Thermoelastic damping.
18. L. LAUDAU and E. LIFSHITZ 1986 *Theory of Elasticity*. New York: Pergamon Press.
19. B. ARMSTRONG 1984 *Geophysics* **49**, 1032–1040. Models for thermoelastic attenuation of waves in heterogeneous solids.
20. V. KINRA and K. MILLIGAN 1994 *American Society of Mechanical Engineering Journal of Applied Mechanics* **61**, 71–76. A second law analysis of thermoelastic damping.
21. K. MILLIGAN and V. KINRA 1993 *Mechanics Research Communications*. On the damping of a one-dimensional inclusion in a uniaxial bar.
22. J. BISHOP and V. KINRA 1992 M3D: *Mechanics and Mechanisms of Material Damping*, American Society for Testing Materials STP 1169, *American Society for Testing and Materials*, *Philadelphia*, *Pennsylvania*, (V. K. Kinra and A. Wolfenden, editors). 457–470. Some improvements in the flexural damping measurement technique.
23. J. BISHOP and V. KINRA 1993 *Journal of Reinforced Plastics and Composites* **12**, 210–226. Thermoelastic damping of a laminated beam in flexure and extension.
24. J. BISHOP and V. KINRA 1993 *Thermodynamics and the Design and Improvement of Energy Systems AES*-Vol. 30, HTD-Vol. 266, (H. J. Richter, editor). *Proceedings of the* 1993 *Winter Annual Meeting*, Elastothermodynamic damping of metal-matrix composites, 127–138.
25. K. MILLIGAN and V. KINRA 1993 Thermodynamics and the Design and Improvement of Energy Systems AES-Vol. 30, HTD-Vol. 266, (H. J. Richter, editor), *Proceedings of the* 1993 *Winter Annual Meeting*. Elastothermodynamic damping of fiber-reinforced metal-matrix composites, 139–148.
26. M. ZEMANSKY and R. DITTMAN 1981 *Heat and Thermodynamics*. New York: McGraw-Hill, sixth edition.
27. D. FREDERICK and T. S. CHANG 1972 *Continuum Mechanics*. Cambridge, MA: Scientific Publishers, 169.
28. W. NOWACKI 1962 *Thermoelasticity*. Oxford: Pergamon Press.
29. OZISIK, M. NECATI 1993 *Heat Conduction*. New York: Wiley, second edition.

30. J. BISHOP and V. K. KINRA 1994 *American Society of Mechanical Engineering. Elastothermodynamic damping in particle-reinforced metal-matrix composites*, AES-Vol. **33**.
31. B. D. COLEMAN and W. NOLL 1961 *Review of Modern Physics* **33**, 239–249. Foundations of linear viscoelasticity.
32. B. D. COLEMAN and V. J. MIZEL 1964 *Journal of Chemistry and Physics* **40**, 1116–1125. Existence of caloric equations of state thermodynamics.
33. S. TIMOSHENKO and J. N. GOODIER 1951 *Theory of Elasticity*. New York: McGraw-Hill, second edition.
34. A. BEJAN 1982 *Entropy Generation Through Heat and Fluid Flow*. New York: John Wiley & Sons.
35. M. GOUY 1889 *Journal of Physics* **8**, 501. Sur l'energie utilisable.
36. A. STODOLA 1910 *Steam and Gas Turbines*. New York: McGraw-Hill.
37. A. DIMAROGONAS 1996 *Vibration for Engineers*. Englewood Cliffs, NJ: Prentice-Hall, second edition.
38. S. N. ZHURKOV and B. N. NARZULLAEV 1953 *Zhurnal Teckhnichescoi Fiziki* **23**, 167. The time-dependence of solids strength (in Russian).
39. S. N. ZHURKOV 1965 *International Journal of Fracture Mechanics* **1**, Kinetic concept of the strength of solids.
40. AtoHaas North America Inc., 100 Independence Hall West, Philadelphia, PA 19106 *General Information and Physical Properties*, Plexiglas, Acrylic Sheet, 1994.
41. G. C. PAPANICOLAOU, A. MARCHESE and P. S. THEOCHARIS 1980 *Journal of Rheology* **24**, 815–828. Thermal and dynamic behavior of the necked region in polycarbonate.
42. J. P. HOLMAN 1990 *Heat Transfer*, New York: McGraw-Hill, seventh edition.
43. E. P. CHEN, G. D. GUPTA, P. D. HILTON, S. L. HUANG, B. MACDONALD, G. C. SIH, R. P. WEI 1972 *Lehigh University, Bethlehem, PA*, 18 015. Applications of Fracture Mechanics to Engineering Problems.
44. S. D. PANTELIOU and A. D. DIMAROGONAS 1997 *Journal of Sound and Vibration* **201**, 555–565. Thermodynamic damping in porous materials with ellipsoidal cavities.
45. S. D. PANTELIOU and A. D. DIMAROGONAS 1997 *Journal of Shock and Vibration* **4**, 261–268. Thermodynamic damping in porous materials with spherical cavities.